Start-to-End Beam Dynamics Simulation

Ji Qiang

Lawrence Berkeley National Laboratory

International Workshop on Future Linear Collider

May 15-19, 2023

Outline

- Introduction
- Computational model
- A start-to-end simulation example
- Further developments needed

Introduction

- Start-to-end simulation provides:
  - Direct evaluation of final beam quality
  - Opportunity for global optimization
  - Testbed for machine imperfection study

Governing Equations in the Start-To-End Simulation

$$\frac{\partial f(r,p,t)}{\partial t} + \dot{r}\frac{\partial f(r,p,t)}{\partial r} + \dot{p}\frac{\partial f(r,p,t)}{\partial p} = 0$$

$$\dot{\vec{r}} = \frac{\partial H}{\partial \vec{p}} \qquad \dot{\vec{p}} = -\frac{\partial H}{\partial \vec{r}}$$

$$H \doteq H_{ext} + H_{sc}$$

$$\nabla^2 \phi = -\rho / \varepsilon$$

$$\rho = \iiint f(r,p,t) d^3 p$$

An Example of the External RF Standing Wave Fields

$$\mathbf{E} = -\frac{\partial \mathbf{A}}{\partial t}$$

$$\mathbf{B} = \nabla \times \mathbf{A}$$

Standing wave cavity with azimuthal symmetry:

$$A_x = \frac{1}{\omega} x \sum_{n=0}^{1} \frac{1}{2(n+1)} e_n^{'}(z) r^{2n} \sin(\omega t + \theta\ )$$

$$A_y = \frac{1}{\omega} y \sum_{n=0}^{1} \frac{1}{2(n+1)} e_n^{'}(z) r^{2n} \sin(\omega t + \theta\ )$$

$$A_z = -\frac{1}{\omega} \sum_{n=0}^{n=1} e_n(z) r^{2n} \sin(\omega t + \theta\ )$$

$$e_{n+1} = -\frac{1}{4(n+1)^2} (e_n^{''}(z) + \frac{\omega^2}{c^2} e_n(z))$$

A Single Step in the Particle-In-Cell Method

$$f = \sum w_i \delta(r - r_i)(p - p_i)$$

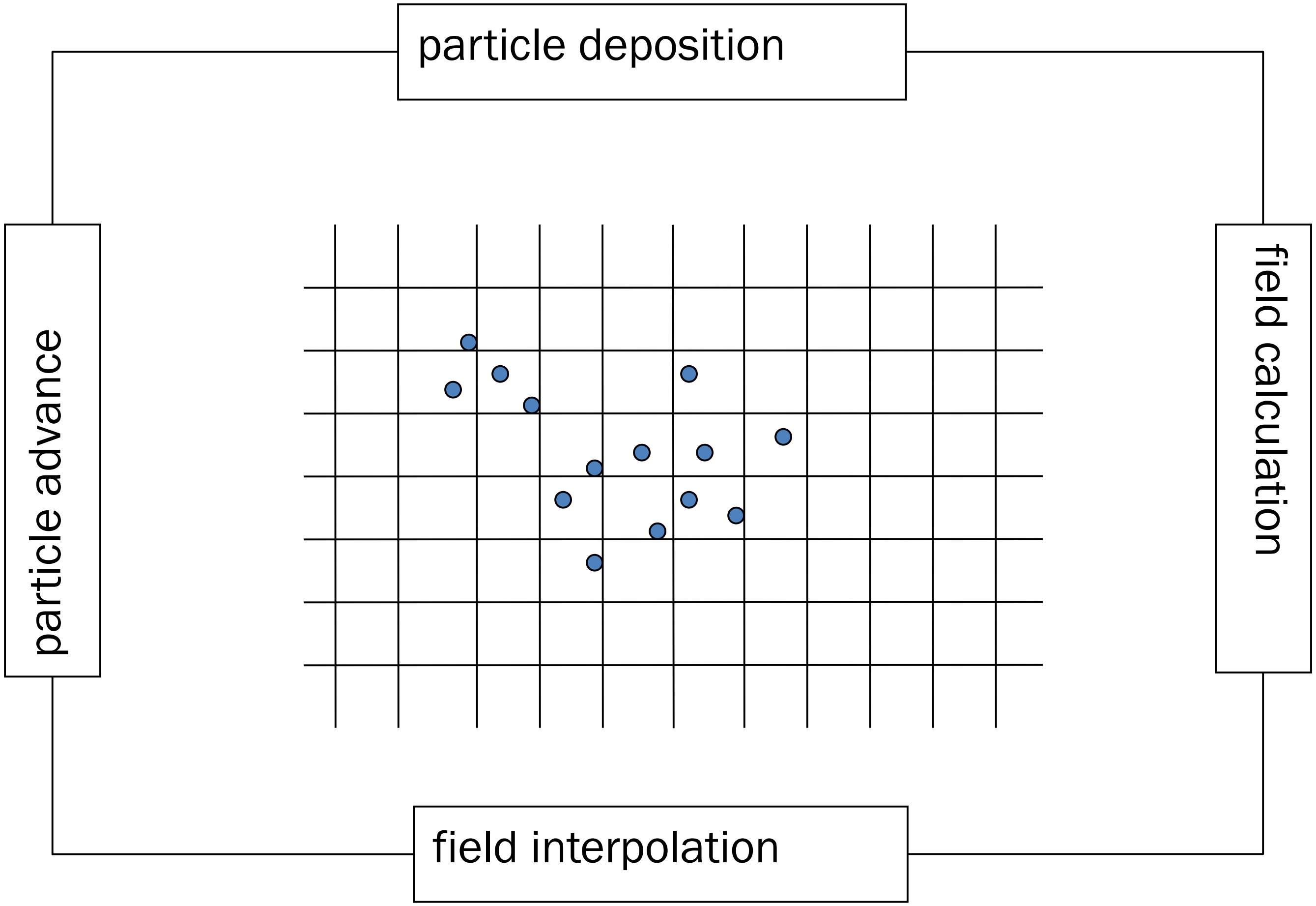

Space-Charge Fields Can be Obtained from Green's Function Solution of Poisson's Equation (I)

$$\phi(r) = \int G(r, r')\rho(r')dr' \qquad ; \; r = (x, y, z)$$

$$\phi(r_i) = h \sum_{i'=1}^{N} G(r_i - r_{i'})\rho(r_{i'})$$

$$\boxed{G(x, y, z) = 1/\sqrt{(x^2 + y^2 + z^2)}}$$

Direct summation of the convolution scales as N^2 !!!!

N – total number of grid points

FFT based Hockney's Algorithm /zero padding:- *scales as (2N)log(2N)*

- Ref: Hockney and Easwood, ***Computer Simulation using Particles***, McGraw-Hill Book Company, New York, 1985.

$$\phi_c(r_i) = h \sum_{i'=1}^{2N} G_c(r_i - r_{i'})\rho_c(r_{i'})$$

$$\phi(r_i) = \phi_c(r_i) \quad \text{for i} = 1, \text{N}$$

Integrated Green Function Method (II)
(large aspect ratio beam with open boundary conditions)

$$\phi_c(r_i) = \sum_{i'=1}^{2N} G_i(r_i - r_{i'})\,\rho_c(r_{i'})$$

$$G_i(r,r') = \int G_s(r,r')\,dr'$$

integrated Green function

$$G_s(x,y,z) = 1/\sqrt{(x^2+y^2+z^2)}$$

standard Green function

Integrated Green's function is needed for modeling large aspect ratio beams!

(O(N log N))

J. Qiang, S. Lidia, R. D. Ryne, and C. Limborg-Deprey, Phys. Rev. ST Accel. Beams, vol 9, 044204 (2006); Phys. Rev. ST Accel. Beams, 10, 129901 (2007).

Comparison between the IG and SG for a beam with aspect ratio of 30

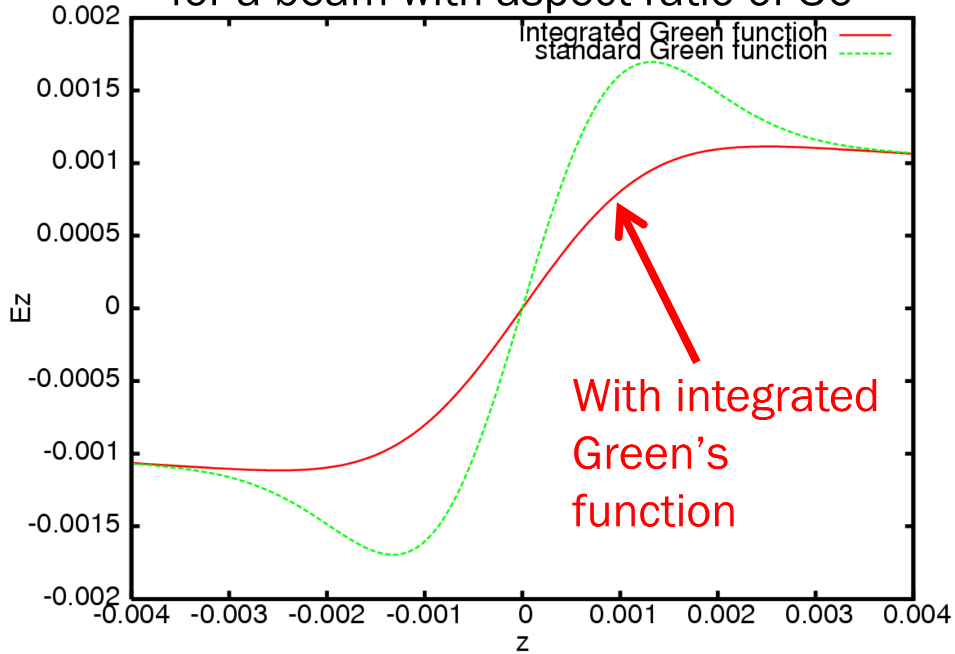

Shifted Green's Function Can Be Used to Find the Image Space-Charge Effects

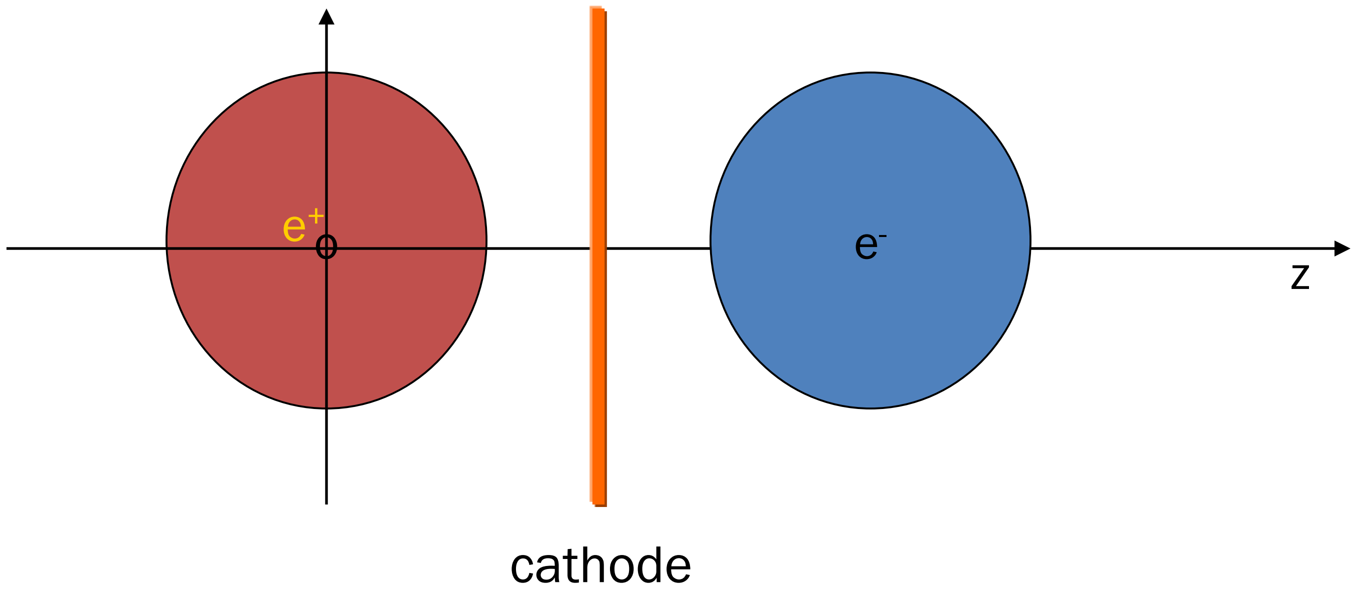

<u>Shifted Green function Algorithm</u>:

$$\phi_F(r) = \int G_s(r, r')\rho(r')dr'$$

$$G_s(r, r') = G(r + r_s, r')$$

J. Qiang, M. Furman, and R. Ryne, Phys. Rev. ST Accel. Beams, vol 5, 104402 (October 2002).

Test of Image Space-Charge Calculation
Numerical Solution vs. Analytical Solution

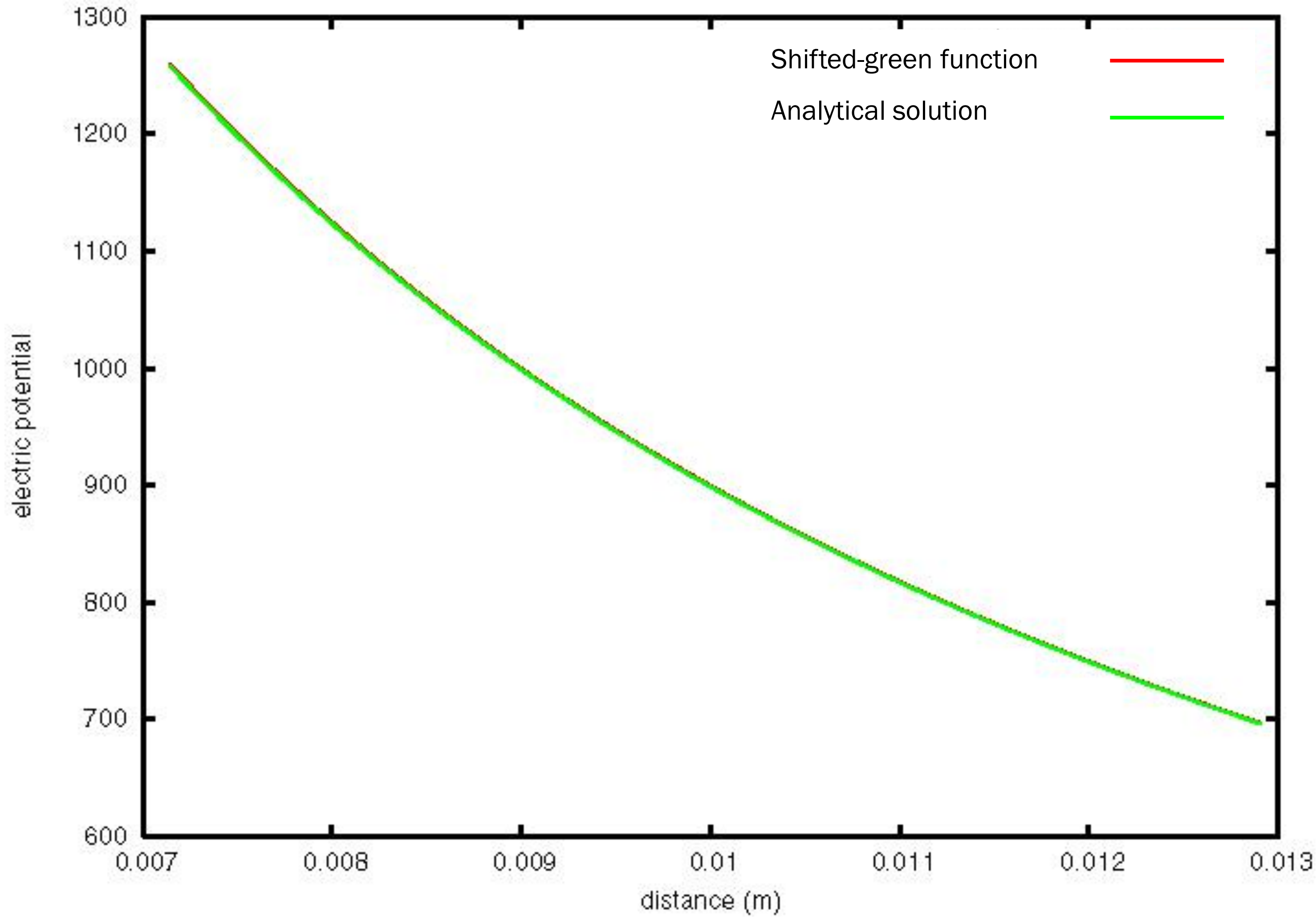

Calculation Longitudinal and Transverse Wakefield Using FFT

$$F_x(s) = q\int_s^{+\infty} W_T(s-s')x(s')\lambda(s')ds'$$

$$F_z(s) = \int_s^{+\infty} W_L(s-s')\lambda(s')ds'$$

$$F(s) = \int_{-\infty}^{+\infty} G(s-s')\rho(s')ds'$$

$$G(s) = \begin{cases} W(s) & for\ s \geq 0 \\ 0 & for\ s < 0 \end{cases}$$

$$F_c(s_i) = h\sum_{i'=1}^{2N} G_c(s_i - s_{i'})\rho_c(s_{i'})$$

$$F(s_i) = F_c(s_i) \quad for\ i = 1,\ldots N$$

Computing Operation Comparison between the Direct Summation and the FFT Based Method

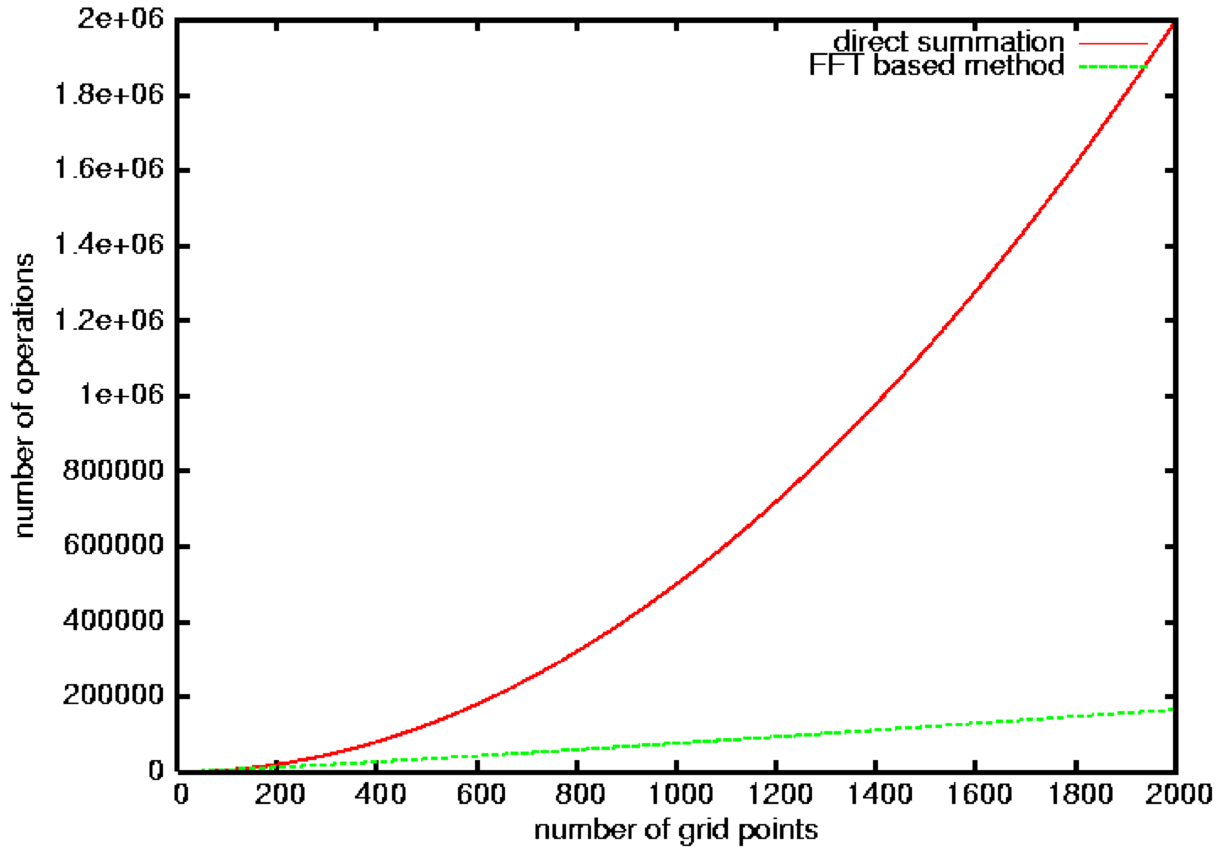

Longitudinal and Transverse Wake Function Examples

The transverse and longitudinal wake functions can be calculated following some analytical expressions or be read in from external files. For analytical representation, the transverse and longitudinal wake functions for the SLAC $2\pi/3$ DDS structure is given by [2]

$$W_T(s) = \frac{4Z_0 c s_0}{\pi a^4}\phi(s)(1-(1+\sqrt{s/s_0}\exp(-\sqrt{s/s_0}))) \tag{10}$$

$$W_L(s) = \frac{Z_0 c}{\pi a^2}\phi(s)\exp(-\sqrt{s/s_{00}}) \tag{11}$$

with

$$s_0 = 0.169\frac{a^{1.79}g^{0.38}}{L^{1.17}} \tag{12}$$

$$s_{00} = \frac{g}{8}(\frac{a}{\alpha(g/L)L})^2 \tag{13}$$

$$\alpha(s) = 1-\alpha_1\sqrt{s}-(1-2\alpha_1)s \tag{14}$$

with $\alpha_1 = 0.4648$. Here, the structure parameters are iris radius a, gap g, period L, and $Z_0 = 120\pi$, $\phi(s)$ is a step function of s ($\phi(s) = 1$ for $s > 0$, 0 for $s < 0$). For the BTW accelerating structure at the ELETTRA linac, the transverse and longitudinal wake functions are [3]

$$W_T(s) = 2.8\times10^{16}\phi(s)((1-(1+\sqrt{s/1.2\times10^{-4}}\exp(-\sqrt{s/1.2\times10^{-4}})))+0.5\sqrt{s}) \tag{15}$$

$$W_L(s) = 1.0\times10^{12}\phi(s)(1226\exp(-\sqrt{s/3\times10^{-4}})+\frac{0.494}{\sqrt{s}}+494\sqrt{s}) \tag{16}$$

1D CSR Wake Field Including Transient Effects

$$\frac{dE(s,\phi)}{cdt} = -\frac{2e^2}{4\pi\epsilon_0 3^{1/3} R^{2/3}}\left(\int_{s-s_L}^{s} \frac{1}{(s-s')^{1/3}}\frac{\partial\lambda(s')}{\partial s'}ds' + \frac{\lambda(s-s_L)-\lambda(s-4s_L)}{s_L^{1/3}}\right)$$

$$W(s) = \begin{cases} -\frac{4}{R}\frac{1}{(\phi_m+2x)}\lambda(s-\frac{R}{6}\phi_m^2(\phi_m+3x)) & for\ source\ in\ front\ of\ the\ bend \\ \frac{4}{R}\left(\frac{\lambda(s-\Delta s_{max}}{(\phi_m+2x)}+\int_{s-\Delta s_{max}}^{s}\frac{1}{\psi+2x}\frac{\partial\lambda}{\partial s'}ds'\right) & for\ source\ inside\ the\ bend \end{cases}$$

$$s - s' = \frac{R\psi^3}{24}\frac{\psi+4x}{\psi+x}$$

Ref: 1) E. L. Saldin, E. A. Schneidmiller, and M. V. Yurkov,
Nucl. Instrum. Methods Phys. Res., Sect. A398, 373 (1997).
2) M. Borland, Phys. Rev. Sepecial Topics - Accel. Beams 4, 070701 (2001).
3) G. Stupakov and P. Emma, ``CSR Wake for a Short Magnet in Ultrarelativistic Limit,"
SLAC-PUB-9242, 2002.

Test of the CSR Wake Implementation for a Short Bend

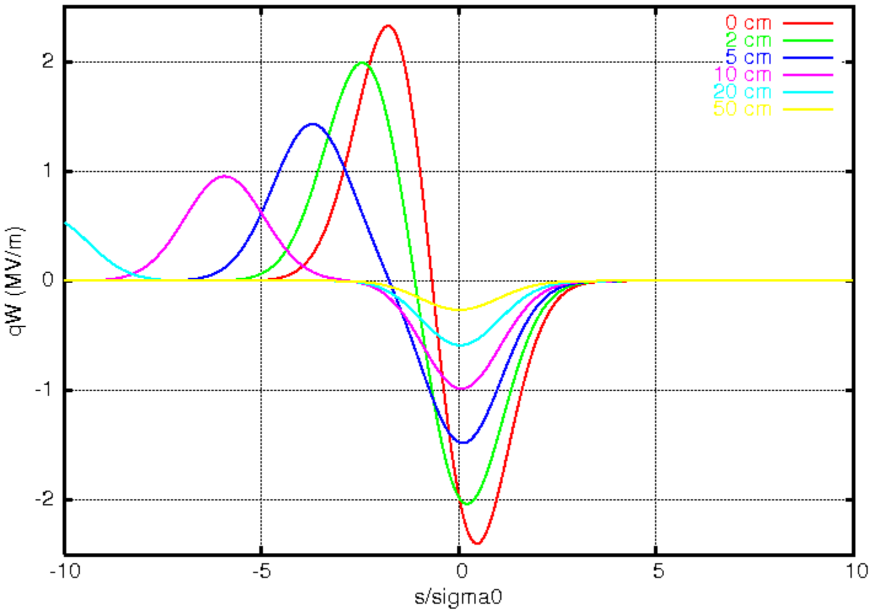

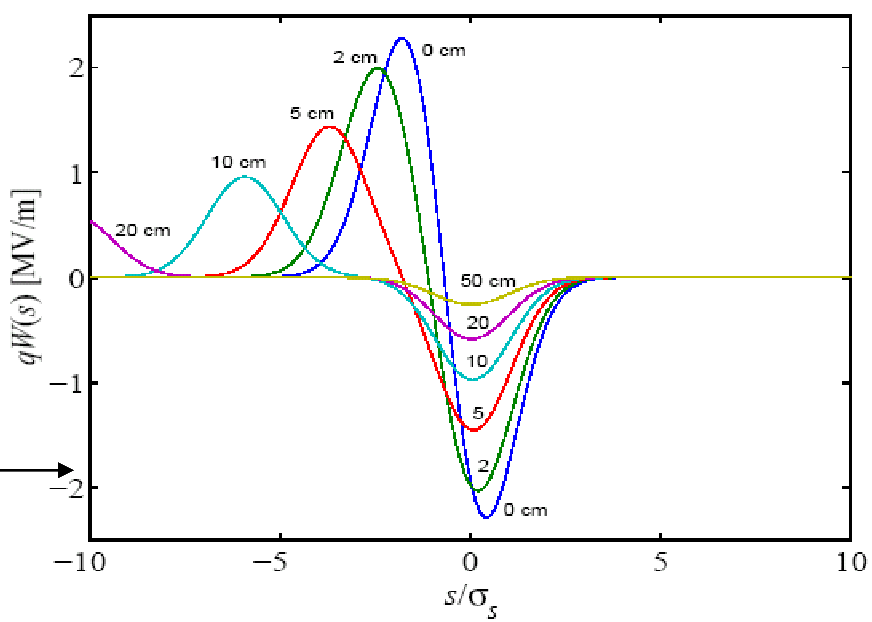

R = 1.5 m, Arc=10 cm

From G. Stupakov and P. Emma

IMPACT-T (https://github.com/impact-lbl/IMPACT-T)

- Parallel PIC code using time "t" as the independent variable

- Key Features
  - Detailed RF accelerating and focusing model
  - Multiple Poisson solvers
    - 3D Integrated Green Function
    - point-to-point
  - Multiple species
  - Monte Carlo gas ionization model
  - Cathode image effects
  - Wakes
  - CSR (1D)
  - Run on both serial and multiple processor computers

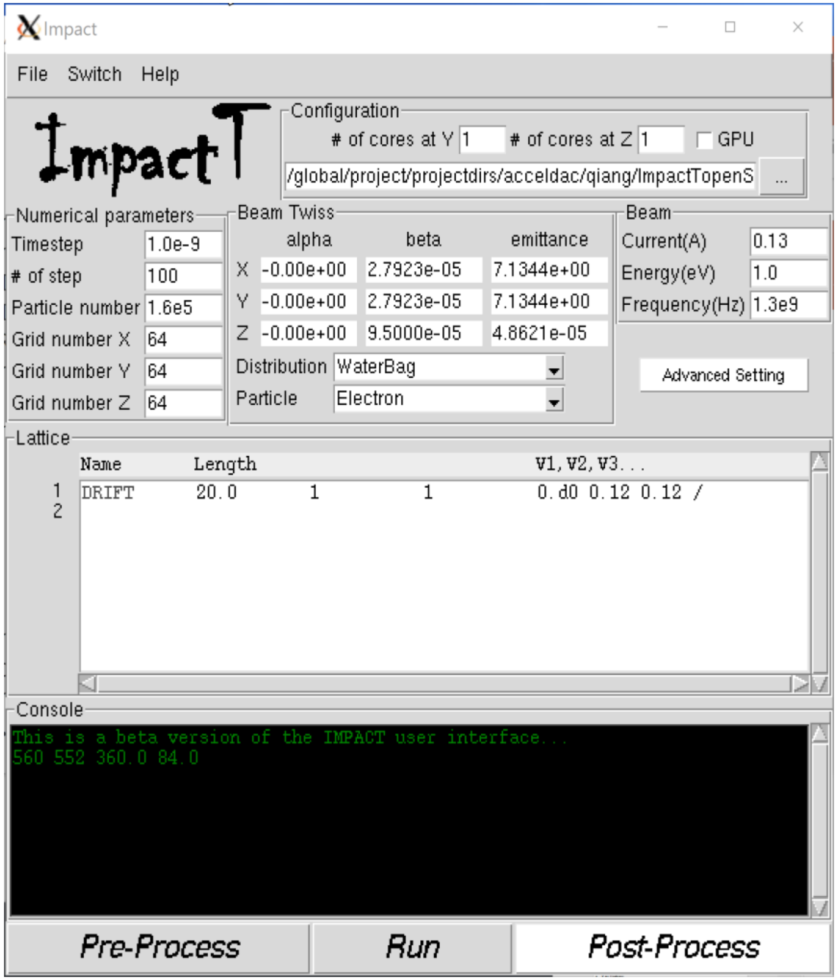

IMPACT-Z (https://github.com/impact-lbl/IMPACT-Z)

- Parallel PIC code using coordinate "z" as the independent variable
- Key Features
  - —Detailed RF accelerating and focusing model
  - —Multiple 3D Poisson solvers
    - Variety of boundary conditions
    - 3D Integrated Green Function
  - —Multi-charge state
  - —Machine error studies and steering
  - —Wakes
  - —CSR (1D)
  - —Run on both serial and multiple processor computers

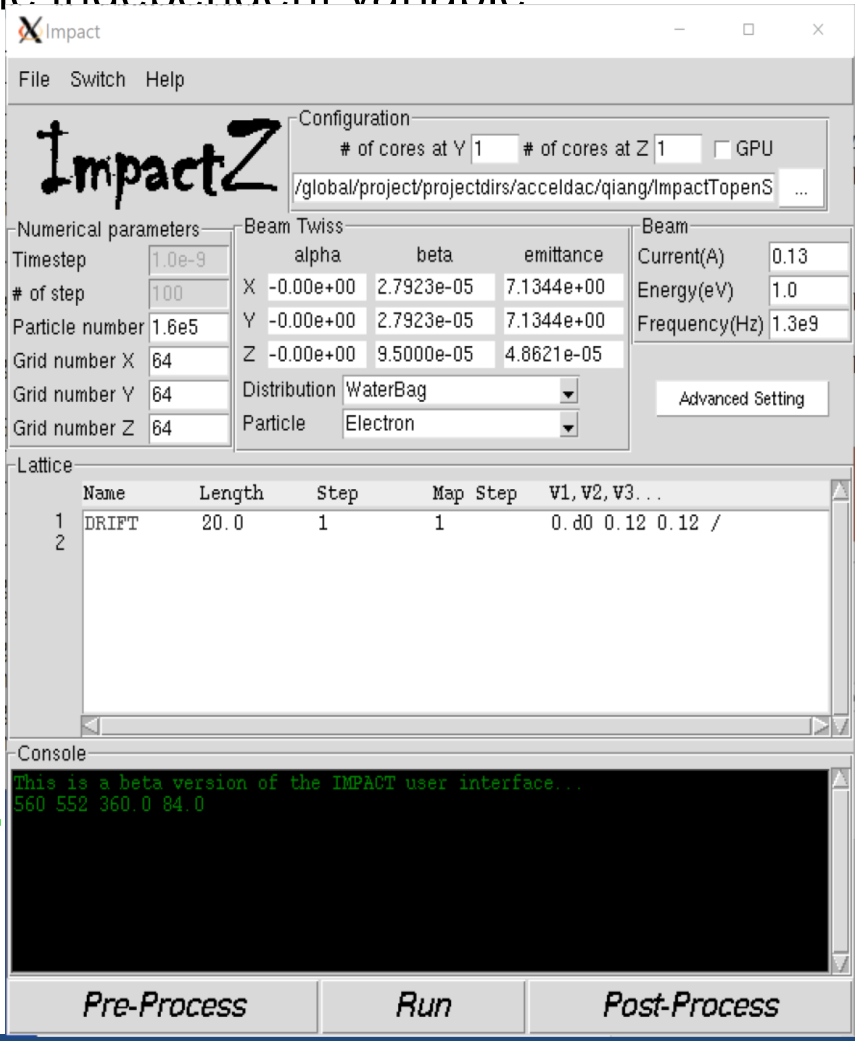

Benchmark of Impact-T Simulations with Experimental Measurements Shows Good Agreement

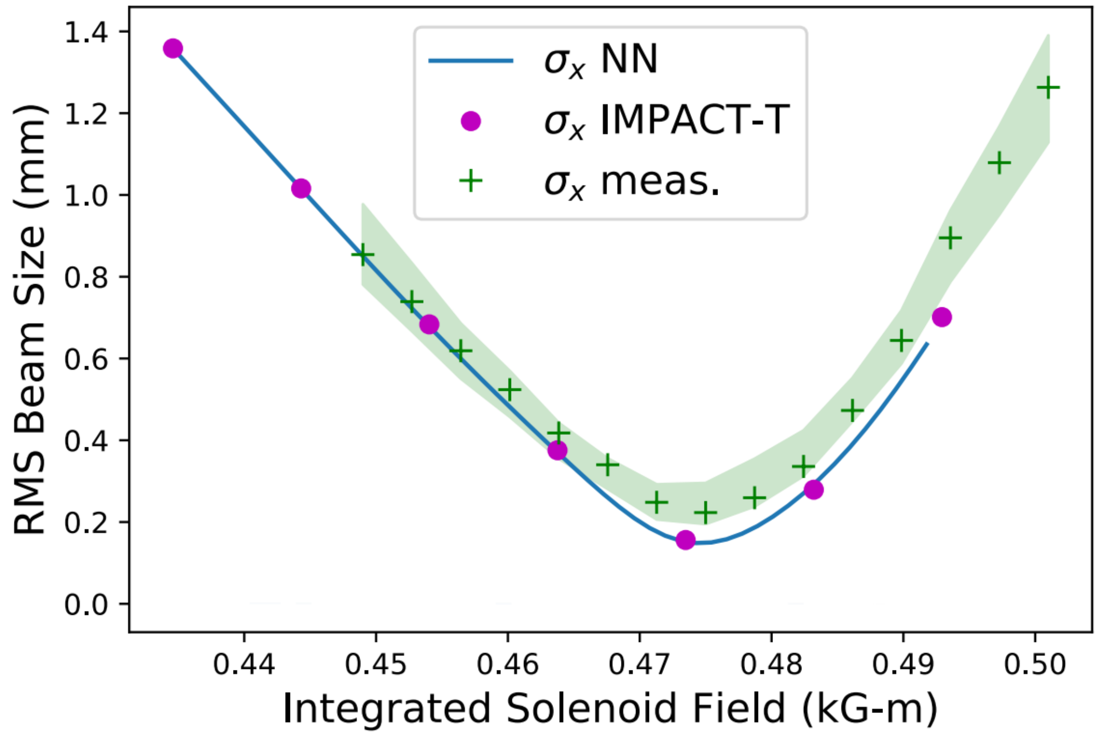

Courtesy of A. Edelen, 2022.

Start-to-End High Fidelity Simulation Reproduces Experimental Observation of MicroBunching at LCLS

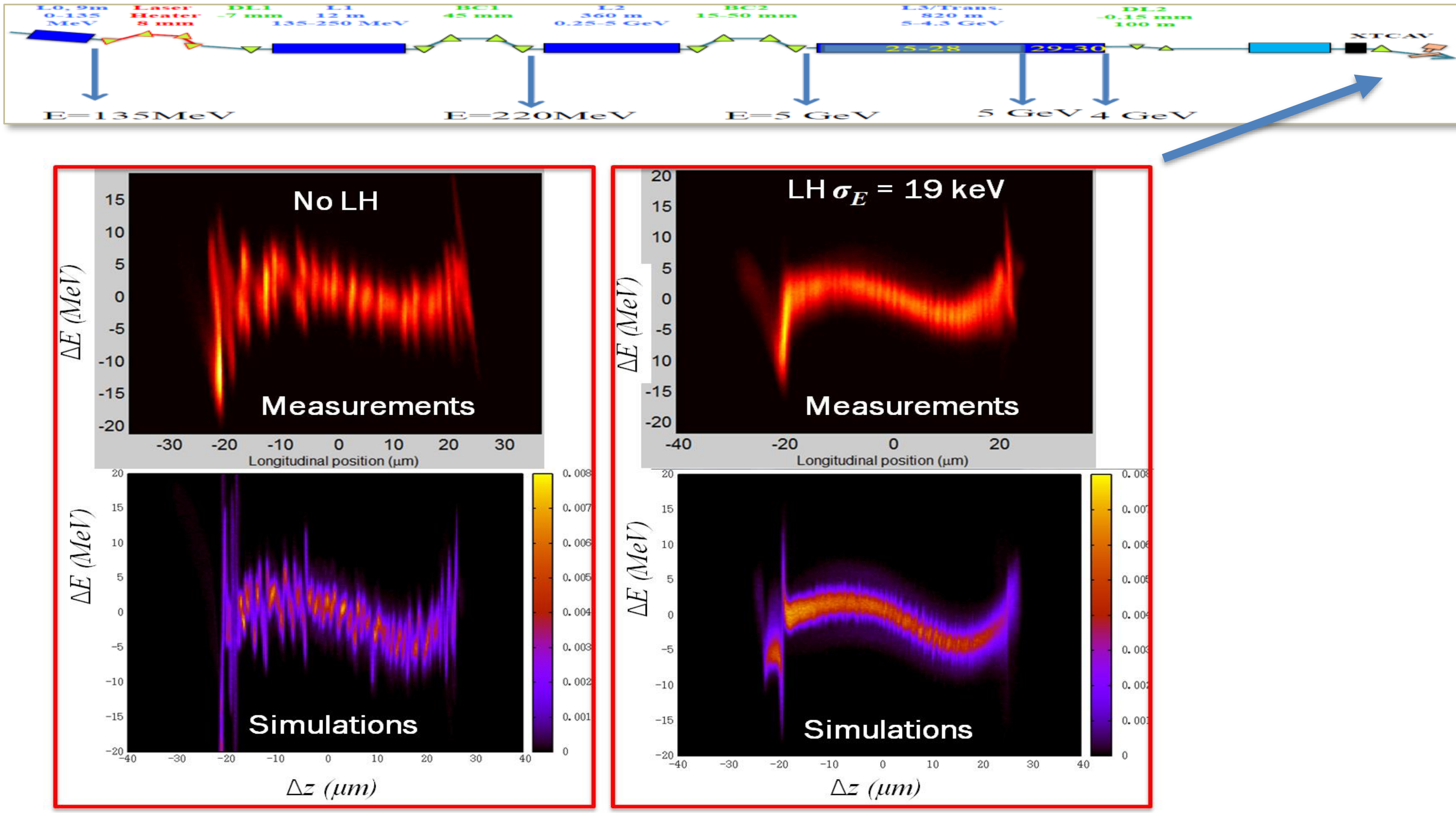

J. Qiang et al., Phys. Rev. Accel. Beams 20, 054402 (2017).

LCLS-II Accelerator Layout
New Superconducting Linac

- Two sources: MHz rate SCRF linac and 120 Hz Cu LCLS-I linac
- Hard and Soft X-ray undulators can operate simultaneously in any mode

Undulator	SC Linac (up to 1 MHz)	Cu Linac (up to 120Hz)
Soft X-ray	0.20 - 1.3 keV with >100 Watts	
Hard X-ray	1.0 - 5.0 keV with >20 Watts	1 - 25 keV with mJ-class X-ray pulses

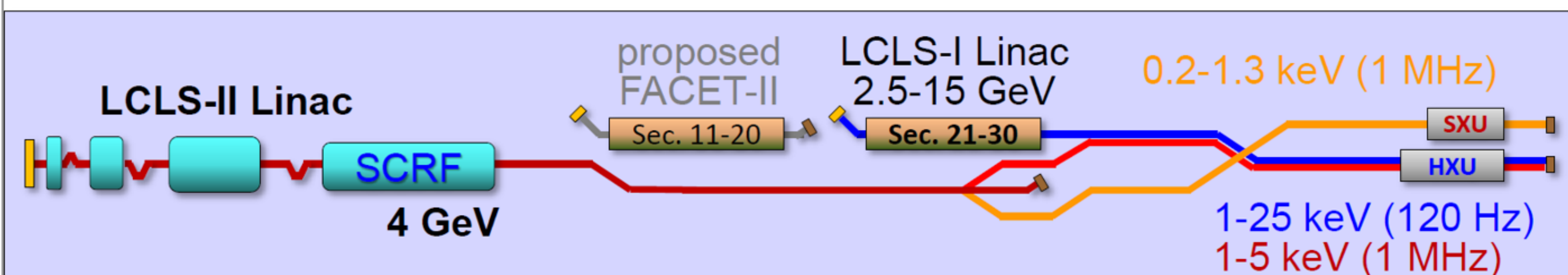

courtesy of T. Raubenheimer

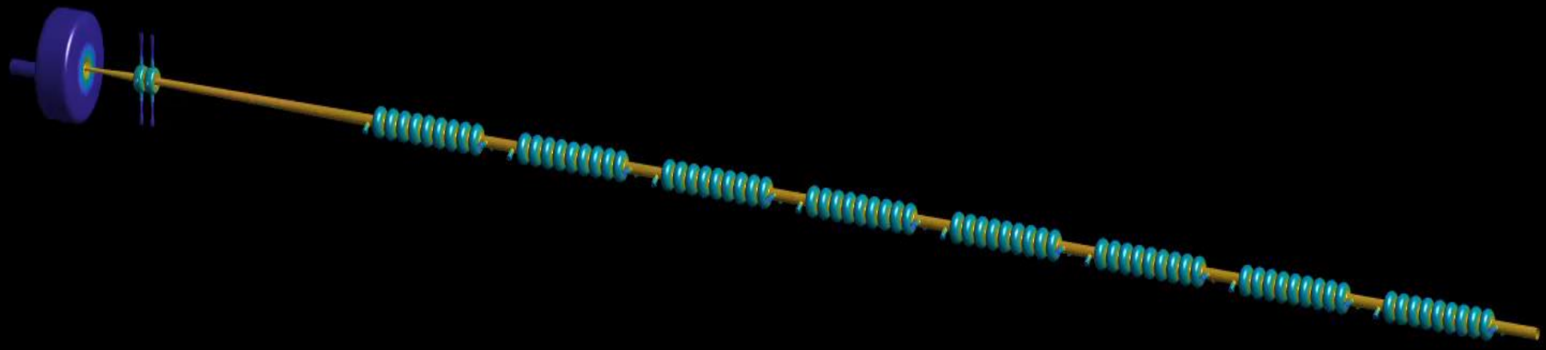

Global Start-to-End Beam Dynamics Optimization Is Needed to Achieve the "Best" Electron Beam Quality

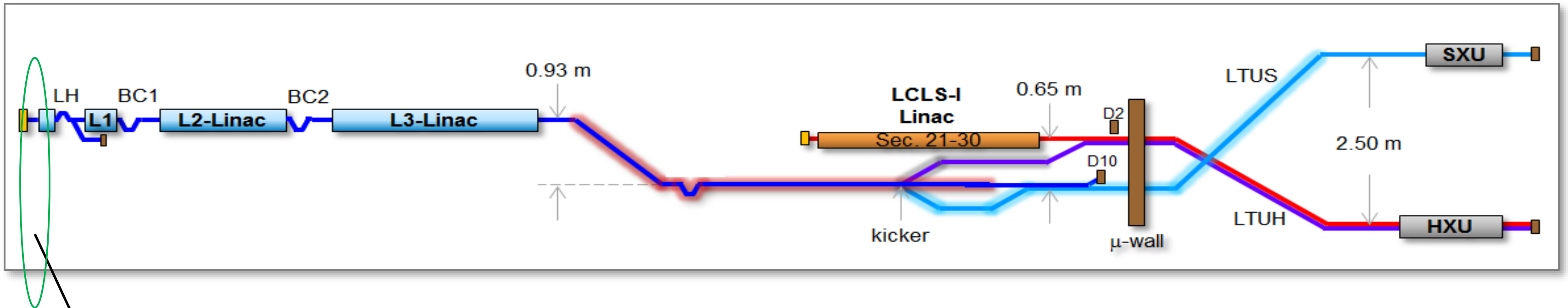

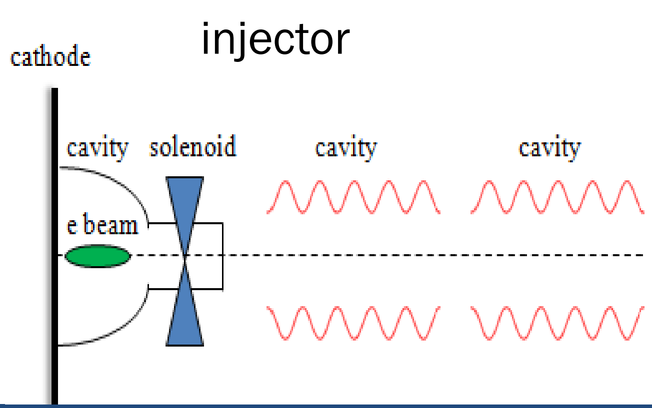

- a best solution from injector does not guarantee the best solution at the end of the accelerator
- global start-to-end optimization enables simultaneous variation of both injector and linac parameters
- local optima may exist given the high dimension of search space
- global optimization method avoids local optimal solutions

Integration of Self-Consistent Beam Dynamics Simulation Using the IMPACT Code with the New Optimization Algorithm for Global Machine Design Optimization

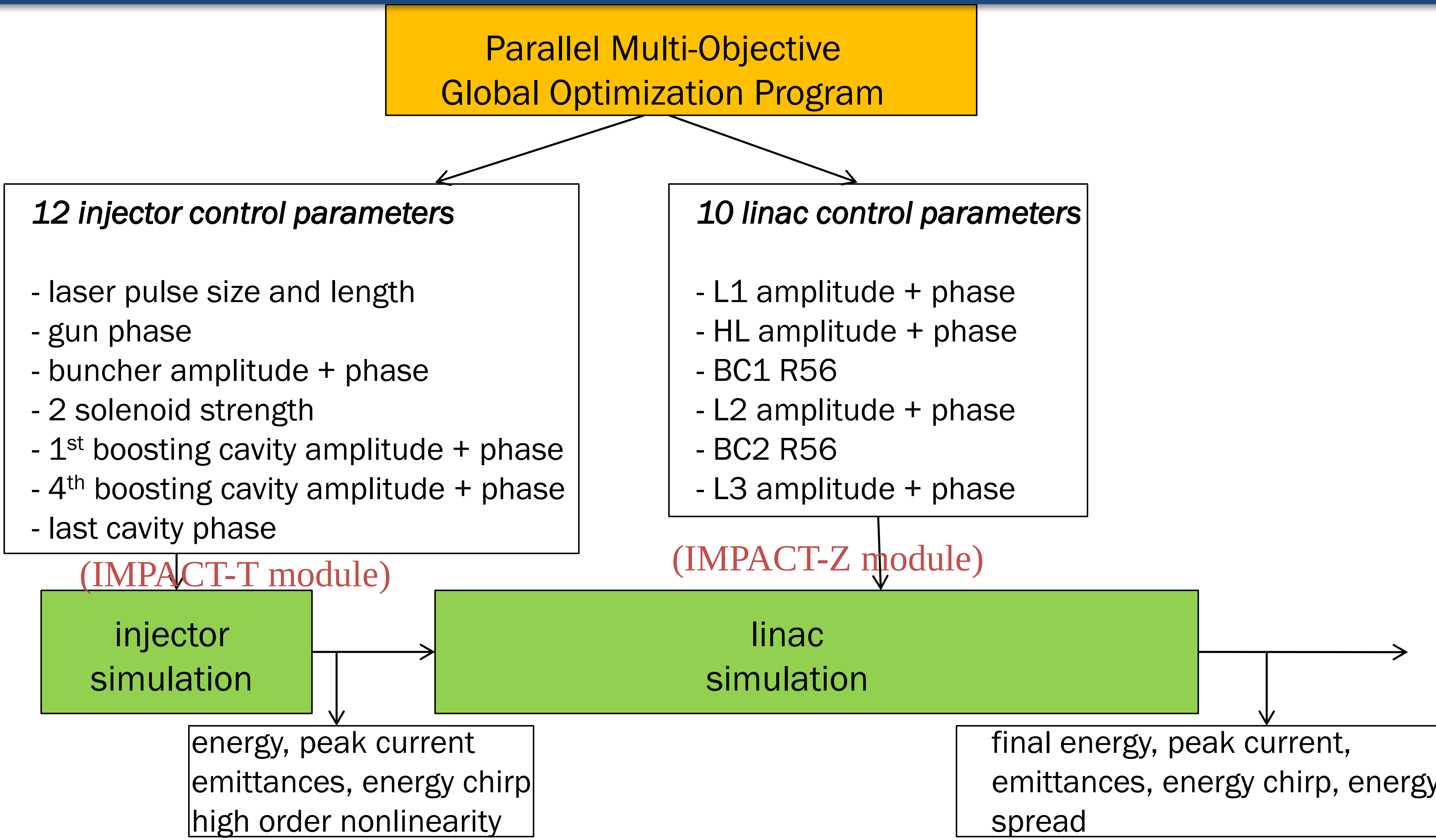

Global Optimization Significantly Improves Accelerator Performance in the LCLS-II Design Application (20 pC Charge)

Pareto front in the Injector Optimization

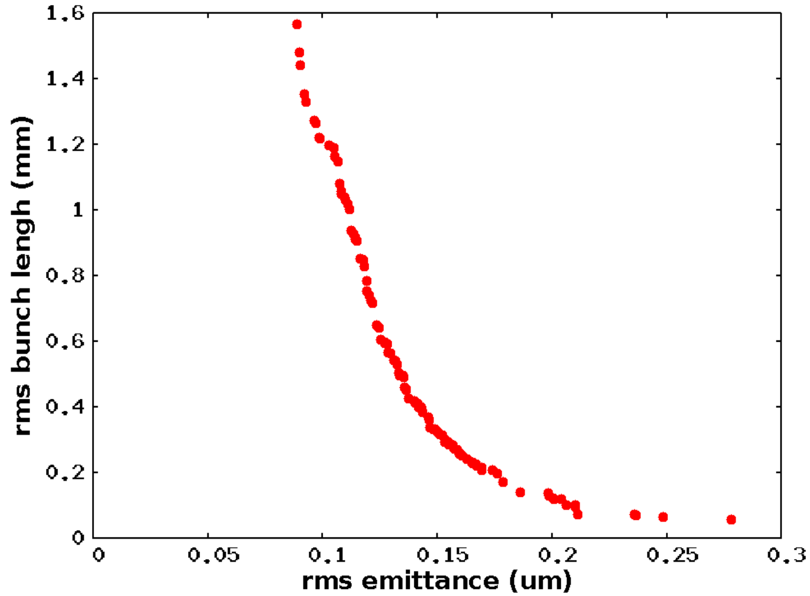

22 Control Parameters:
- 12 in the injector
- 10 in the linac

final Pareto front solutions

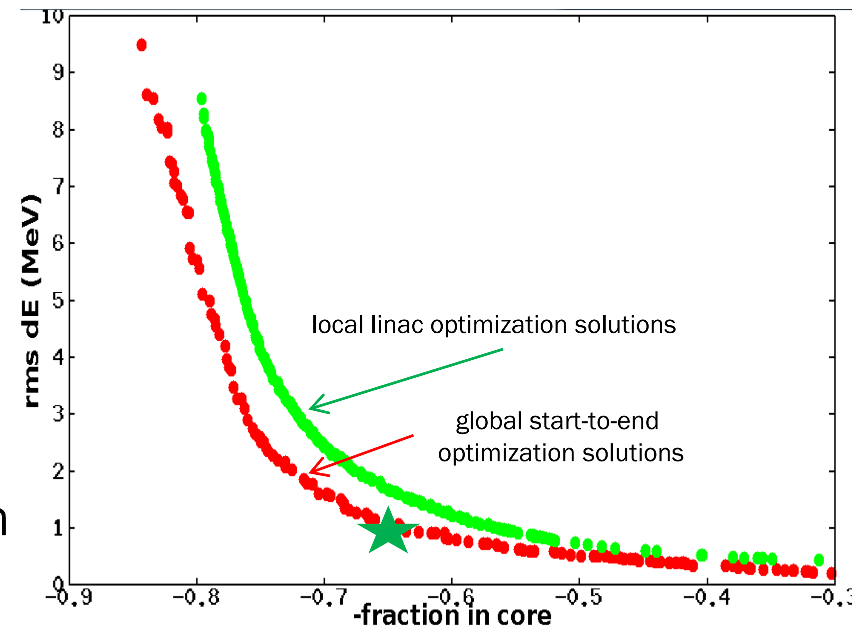

- Global optimization shows significantly better solutions than the local optimization

J. Qiang, in proceedings of NA-PAC 2016.

Global Optimization Improves Final Electron Beam Quality and Results in 50% X-Ray Radiation Energy Improvement (20pC)

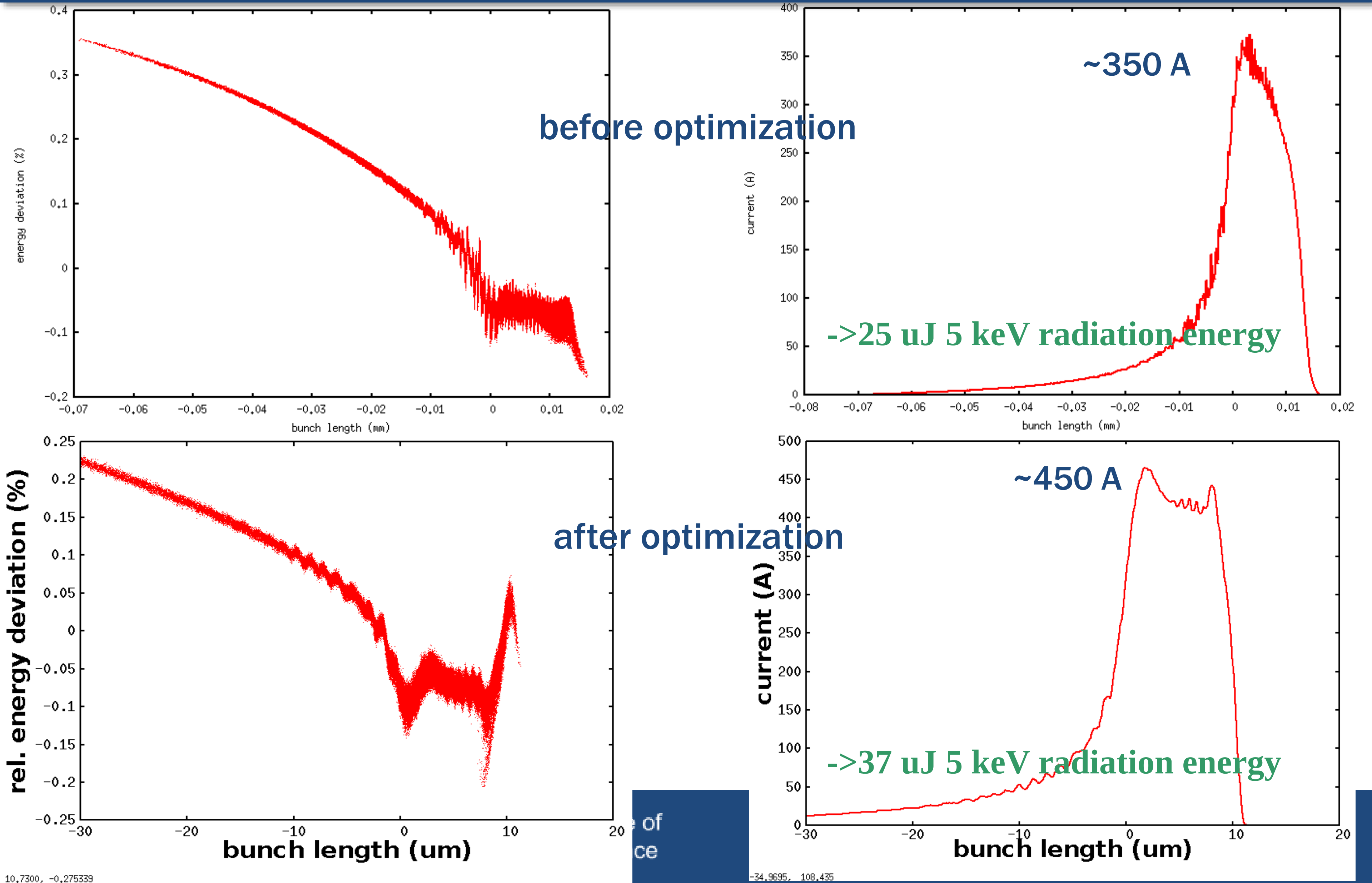

Further Developments Needed

- Long-range wakefield effects
- Beam-beam interaction with beamstrahlung effects
- Modeling of polarization
- Other potential effects